A New Approach to the Generation of Retractable Plate Structures Based on One-Uniform Tessellations

Aylin Gazi Gezgin
Department of Architecture,
Izmir Institute of Technology,
Gulbahce Koyu Kampusu,
Urla, Izmir 35430, Turkey
e-mail: aylingazi@msn.com

Koray Korkmaz[1]
Department of Architecture,
Izmir Institute of Technology,
Gulbahce Koyu Kampusu,
Urla, Izmir 35430, Turkey
e-mail: koraykorkmaz@iyte.edu.tr

Retractable plate structure (RPS) is a family of structures that is a set of cover plates connected by revolute joints. There exists wide range of possibilities related with these structures in architecture. Configuring the suitable shape of rigid plates that are able to be enclosed without any gaps or overlaps in both closed and open configurations and eliminating the possibility of contact between the plates during the deployment have been the most important issues in RPS design process. Many researchers have tried to find the most suitable shape by using kinematical or empirical analysis so far. This study presents a novel approach to find the suitable shape of the plates and their assembly order without any kinematical or empirical analysis. This approach is benefited from the one-uniform mathematical tessellation technique that gives the possibilities of tiling a plate using regular polygons without any gaps or overlaps. In the light of this technique, the shape of the plates is determined as regular polygons and two conditions are introduced to form RPS in which regular polygonal plates are connected by only revolute joints. It should be noted that these plates are not allowed to become overlapped during deployment and form gaps in closed configuration. Additionally, this study aims to reach a single degree-of-freedom (DoF) RPS. It presents a systematic method to convert multi-DoF RPS into single DoF RPS by using the similarity between graph theory and the duality of tessellation. [DOI: 10.1115/1.4036570]

Keywords: retractable plate structure, tessellation, graph theory, duality, mobility

1 Introduction

Over the last couple of decades, many concepts have been proposed for deployable structures employing bars or plates. Deployable structures based on pantographic elements have wide range of application possibilities in architecture and engineering such as retractable roof, kinetic façade, or even kinetic photovoltaic panels [1–3]. The use of translational and polar pantographic bar elements as a unit element is pioneered by Spanish architects Piñero and Escrig [4] and Escrig and Valcarcel [5]. In early 1990s, Hoberman developed a concept by the invention of angulated elements [2,6]. On the contrary to translational and polar units, angulated elements are formed by two kinked beams. You and Pellegrino extend this concept by substituting simple angulated beams to the multi-angulated beams [7]. Despite the advantages of pantograph structures, few have successfully been realized because design process is complex. Mira designed a new multiconfigurational universal scissor component to develop domes and barrel vaults [8].

The necessity to cover deployable structures has gained importance in time. As a result of durability problem of membrane, many researches have focused on rigid plates to cover the deployable structures. Thus, the suitable shape of rigid plates has been one of the crucial issues for the researchers. Kassabian et al. investigated cover plates that can be attached to the multi-angulated bars [9]. In addition to this approach, Jensen and Pellegrino developed a method for covering any multi-angulated bar structure with plates by finding extreme position of an expandable structure [10]. In their further research, they removed the angulated elements and connected the plates directly with revolute joints exactly the same locations as in the original bar structure [11]. With this concept, Jensen and Pellegrino led to the creation of a family of structures called retractable plate structures. Lou et al. used an analytical approach to derive a set of conditions that can be used to determine whether all of the pivot locations of multi-angulated beams are enveloped by the boundary of its corresponding plate. Designers can choose an opening profile which suits their needs and then apply appropriate formula to determine the edges of the cover plates [12]. Rodriquez and Chilton combined polygonal plates and straight elements in the swivel diagraph. It offered more possibilities of design, employing fewer elements and allowed external fixed support [13]. In addition, Wohlhart proposed moveable planar double-chains with only rotary joints and spatial double-chains held together by gussets. Both types were overconstrained linkages [14]. Wei and Dai proposed a more general single plane symmetric eight-bar linkage to be used in the synthesis and construction of a group of deployable platonic mechanism with radially reciprocating motion [15,16]. Gazi and Korkmaz combined polygonal plates and bars by benefiting tessellation technique to reach an expandable structure [17]. Research on the calculation of mechanism mobility is also important in understanding the accuracy of the design process. Gazi and Korkmaz investigated the mobility analysis of the RPSs [18].On the other hand, Sareh and Guest presented a number of novel concepts and definitions, which help to apply systematic variations on Miura-ori pattern. They reduced the symmetry of the Miura-ori to obtain new patterns [19,20].

It should be noted that all of the studies above include either the assembly of rigid plates solely together or by using additional bar structures between them. On the other hand in both cases, utilizing kinematical synthesis and empirical design methods, researchers aimed to find the suitable shapes of the rigid plates that match perfectly by forming assembly without any gaps or overlaps in their fully closed and open configurations. The aim of this study is to present a new design approach without any kinematical synthesis or empirical design methods. The shapes of the

[1]Corresponding author.

Manuscript received August 12, 2016; final manuscript received March 22, 2017; published online May 24, 2017. Assoc. Editor: Jian S. Dai.

platforms are determined as regular polygons. Thus, this study focuses on one-uniform tessellations technique that gives all the possibilities of assembling regular polygons in the same order on a plane. These one-uniform tessellations will be the closed configurations of RPSs. The layout of the paper begins with the fundamentals of uniform tessellation technique. By considering one-uniform tessellations' geometrical properties, two conditions are presented to design retractable plate structures that are not allowed to overlap and gaps in any configuration. Additionally, this study aims to reach a single DoF RPS and present a systematic conversion of multi-DoF RPS to a single DoF RPS by using graph theory and duality of tessellation.

2 Tessellations

Tessellation is a kind of mathematical technique to cover a surface without any gaps or overlaps and it has been used since ancient times in art and architecture. Architects generally use tessellation technique especially in surface designs such as grounds, façades, and floors. Despite the usage of tessellation since ancient times, the science of tessellation is comparatively recent. In mathematical literature, there are many classifications of tessellation. This study deals with the tessellations that are classified with respect to the polygon shape. In this classification, all the polygons are regular as equiangular and equilateral. Tessellations with regular polygons are usually represented by the number of sides of the polygons around any vertex point written in the clockwise or counterclockwise order [21].

The first important studies about tessellations with regular polygons were conducted by Johannes Kepler. Johannes Kepler mentioned about the regular polygons that are able to cover a plane and he described the regular and semiregular tessellations [22]. Another important development came from Badoureau in 1881. Badoureau determined all the possibilities for regular polygons meeting at a vertex, but he was only interested in monogonal tessellations. The correct determination about the polygons, and vertex figures were done by Sommerville 1905 [23].

The possibilities of edge-to-edge tessellation with regular polygons on a plane can be found by using some formulations. The interior angle at each corner of a regular n-gon $\{n\}$ is $(n-2)/n$ rad or $(180(n-2)/n$ deg). In the light of this formulation, the number of single-type regular polygons that fit a vertex is

$$360/[(n-2)180/n] = 2n/(n-2) = 2 + 4/(n-2) \tag{1}$$

By using this formulation, only regular hexagons, squares, and equilateral triangles can be tessellated. If three different types of regular polygons should fit around a vertex, the formulation is

$$[(n_1-2)/n_1 + (n_2-2)/n_2 + (n_3-2)/n_3]180\,\text{deg} = 360\,\text{deg} \tag{2}$$

If four different types of regular polygons should fit around a vertex, the formulation is

$$1/n_1 + 1/n_2 + 1/n_3 + 1/n_4 = 1 \tag{3}$$

If five different types of regular polygons should fit around a vertex, the formulation is

$$1/n_1 + 1/n_2 + 1/n_3 + 1/n_4 + 1/n_5 = 3/2 \tag{4}$$

If six different types of regular polygons should fit around a vertex, the formulation is

$$1/n_1 + 1/n_2 + 1/n_3 + 1/n_4 + 1/n_5 + 1/n_6 = 2 \tag{5}$$

According to this formulation, 17 different arrangements of regular polygons can fit around a vertex. Four of the arrangements have two distinct ways; so, there are 21 ways to fit the regular polygons around a vertex [24,25]. These vertex combinations are: (3.7.42); (3.8.24); (3.9.18); (3.10.15); (3.12.12); (4.5.20); (4.6.12); (4.8.8) or (4.8^2); (5.5.10); (6.6.6) or (6^3); (3.3.4.12) or $(3^2.4.12)$; (3.4.3.12); (3.3.6.6) or $(3^2.6^2)$; (3.6.3.6); (4.4.4.4) or (4^4); (3.4.4.6) or $(3.4^2.6)$; (3.4.6.4); (3.3.3.3.6) or $(3^4.6)$; (3.3.3.4.4) or $(3^3.4^2)$; (3.3.4.3.4) or $(3^2.4.3.4)$; (3.3.3.3.3.3) or (3^6). However, not all of these can tessellate the plane. In these arrangements, just 11 of them can cover the plane without any gaps or overlaps that are called one-uniform tessellations.

2.1 Uniform Tessellations. In any tessellation, if all vertices are identical and there exists the same combination and arrangement of polygons at each vertex, these tessellations are called one-uniform tessellations. Inside this category, there exist three regular and eight semiregular tessellations (Figs. 1 and 2).

If the combination and the arrangement of regular polygons at each vertex are not the same, these tessellations are called k-uniform tessellations. The enumeration of the k uniform tessellation is proofed by Krötenheerdt [26] by using the fact that the symmetry group of each k-uniform tessellation is one of the 17 different arrangements. The number of k-uniform tessellations are: $k(2) = 20$, $k(3) = 39$, $k(4) = 33$, $k(5) = 15$, $k(6) = 10$, $k(7) = 7$ and totally there exist 135 distinct types of k-uniform tessellations (Fig. 3).

2.2 Duality of Tessellations. The concept of duality occurs in almost every branch of mathematics. While isomorphism preserves certain relations between mathematical entities under consideration, duality reverses them. There is a deeper connection between any tessellation; begin with placing a vertex at the geometric center of each polygon in the original tessellation. For instance, the triangular and hexagonal tessellations are duals of each other, while the square tessellation is its own dual (Fig. 4). The dual of regular tessellations are regular tessellations; however the dual of semiregular tessellations are not regular (Fig. 5).

3 Conditions of RPS Based on One-Uniform Tessellation

In this section, shapes of the plates and their assembly order are determined with respect to the selected one-uniform tessellation. Thus, the plates are regular polygons and connected to each other from the nodes using only revolute joints based on vertex order of selected tessellation. The nodes are the vertices of the polygons. In this section, two conditions will be presented in order to design RPS that can be deployed without any gaps or overlaps. The first condition is about being retractable, and the second condition is about retraction and expansion feature.

Condition 1. To reach a retractable plate structure based on one-uniform tessellation, at least four edges of the tessellation must meet at every vertex.

One-uniform tessellations have the arrangement of the same number of polygons at the vertices. When these polygonal plates are assembled with each other by considering the combination order around every vertex, they constitute a mechanism or a structure. Three plates around a vertex connected with revolute joints constitute a structure. Four or more plates are necessary to constitute a mechanism. Figure 6 represents all one-uniform tessellations,

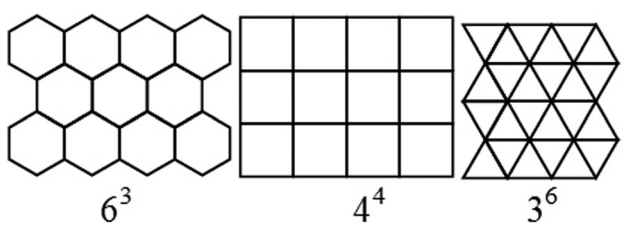

Fig. 1 One-uniform regular tessellations

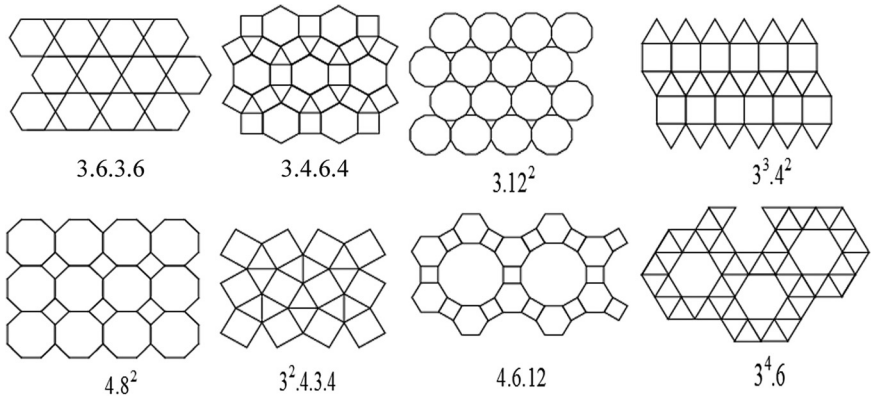

Fig. 2 One-uniform semiregular tessellations

number and order of edges at a vertex, type of rigid plates, and their assembly order. As it can be seen in Fig. 6, four tessellations, (6^3), ($8^2.4$), (3.12^2), (4.6.12), constitute a structure.

In this study, all retractable plates move in planes parallel to one another. All retractable plate structures are a kind of planar mechanisms. For instance, when kinematic behavior of an RPS based on 4^4 tessellation is investigated, it can be seen that RPS expands and retracts in a predictable manner as shown in Fig. 7.

Research on the calculation of mechanism mobility is also significant in understanding the kinematic behavior of RPS. Traditionally, the Grübler's criterion has been used to study mobility in mechanism science [27]. The formula provided by this criterion allows the mobility or number of degrees-of-freedom of a mechanical system to be calculated. According to Grübler's criterion, mobility (M) equals to

$$M = 3(L - 1) - 2j_1 - j_2 \tag{6}$$

where M is total degrees-of-freedom or mobility of the mechanism; L is the number of links; j_1 is the number of lower pairs, which represents kinematic pairs with one degree-of–freedom; and j_2 is the number of higher pairs, which represents kinematic pairs with two degrees-of-freedom. In this study, higher pair is not

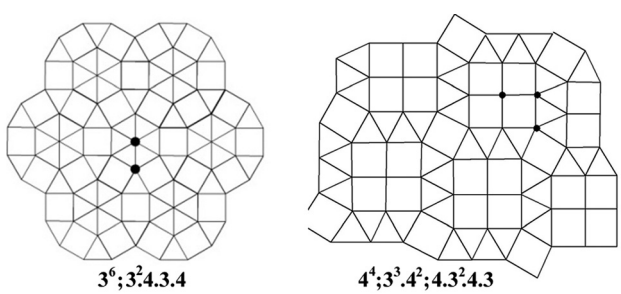

Fig. 3 Examples of *k*(2) and *k*(3) uniform tessellations

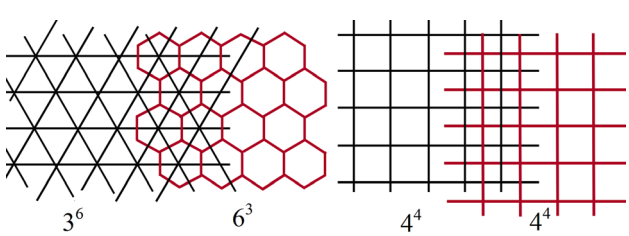

Fig. 4 Dual of regular tessellations

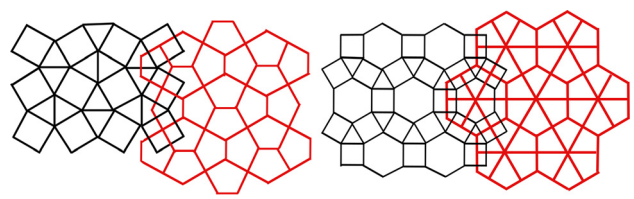

Fig. 5 Dual of semiregular tessellations

1-Uniform Tessellations	Number of edges at a vertex	Type of Rigid Plate	Assembling Order	Chain or Structure
4.4.4.4	4			4 bar chain
6.6.6	3			Structure
3.3.3.3.3.3	6			6 bar chain
3.6.3.6	4			4 bar chain
8.8.4	3			Structure
3.12.12	3			Structure
4.6.12	3			Structure
3.4.6.4	4			4 bar chain
3.3.4.3.4	5			5 bar chain
3.3.3.4.4	5			5 bar chain
3.3.3.3.6	5			5 bar chain

Fig. 6 Movement capability of regular polygons around a single vertex of every one-uniform tessellations

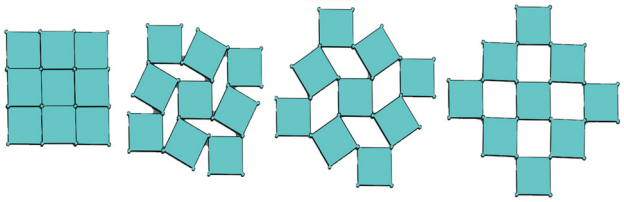

Fig. 7 Expansion of RPS based on 4^4 tessellation

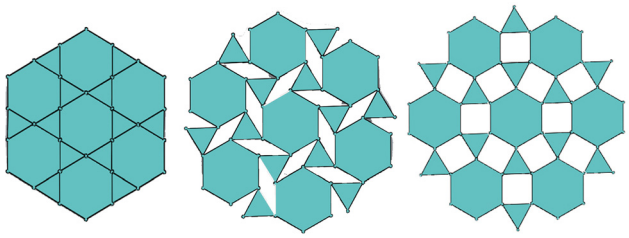

Fig. 8 Expansion of RPS based on (3.6.3.6) tessellation

used. If $M \leq 0$, according to Eq. (6), there exists no movement. It is a structure.

On the other hand, this equation does not hold in some situations. Grübler's equation (Eq. (6)) is only valid for regular planar mechanisms. It fails to provide right mobility answers to the overconstrained mechanisms where the mobilities are different due to the existence of special geometric conditions among the links and joint axes that are referred as overconstrained conditions. For example, in Fig. 7, RPS based on 4^4 tessellation is movable. However, if square tessellation parameters are substituted into Eq. (6) as $L = 9$ and $J_1 = 12$, mobility will be calculated as $M = 3(9-1) - 2.12 = 0$. In Fig. 8, RPS based on (3.6.3.6) tessellation is moveable too. However, if tessellation parameters are substituted into Eq. (6) as $L = 19$, $j_1 = 30$, the mobility of the RPS based on 3.6.3.6 tessellation is calculated as $M = 3(19-1) - 2.30 = -6$.

Many studies focus on this and developed new approaches in terms of mobility calculations [28–30]. As an addition to them, this paper also calculates the mobility of tessellation overconstrained mechanisms by modifying Grübler's criterion by adding the number of excessive links (q) term from Alizade's universal mobility equation [31]

$$M = 3(L-1) - 2j_1 - j_2 + q \tag{7}$$

As seen in Figs. 9 and 10, if square tessellation parameters are substituted into Eq. (7) as $L = 9$, $J_1 = 12$, and $q = 1$, the mobility of the RPS becomes $M = 3(9-1) - 2.12 + 1 = 1$. This result can be applied to the other RPSs based on one-uniform tessellation.

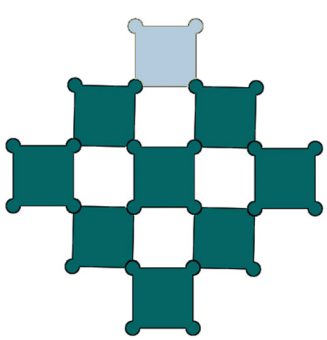

Fig. 9 Simplest module of the RPS based on square tessellation with an excessive plate

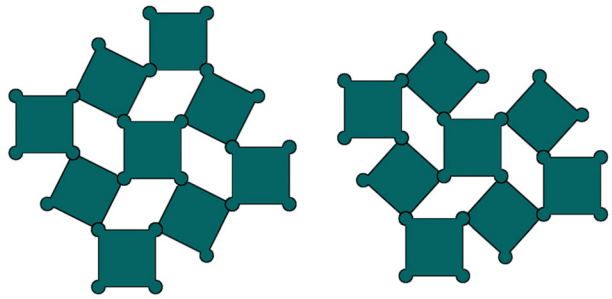

Fig. 10 Simplest module of the RPS based on square tessellation with and without the excessive plate

Proof 1. In order to prove this condition, let us consider a simple closed planar kinematic chain with a single loop and n links (Fig. 11). In order to change its loop form, this kinematic chain should have a mobility (M) higher than zero $M > 0$. Considering this fact and the Grübler's general mobility equation $M = 3(L-1) - 2j_1 - j_2$, minimum number of link requirement can be calculated. As the study focuses on planar tessellations with lower kinematic pairs, mobility equation can be adjusted as $M = 3(L-1) - 2j_1$.

It is clear that to assemble n-rigid links into a single closed loop, n connections are required; if these connections are replaced by the one degrees-of-freedom kinematic pairs, we can formulate the total number of one degrees-of-freedom kinematic pairs (j_1) as $j_1 = n$. Using this information, Grübler's mobility equation for a single closed planar kinematic chain becomes $M = (L-1) - 2n$ $M = n - 3$. In the light of this for the minimum mobility $M = 1$, number of requirement rigid link should be $n = 4$. In other words, to form any mobile loops, at least four rigid bodies are required to be assembled. Using this fact, let us return back to condition 1. In order to have a retractable plate structure based on one-uniform tessellation, each plate should be neighbor of only mobile loops to move individually. Moreover, it is clear that to form a tessellation, every plate should be positioned by edges to edges and corner to corners in their closed form. Thus considering the smallest mobile option, a mobile loop should be formed at least by utilizing four plates and to form a tessellation, these plates should be gathered around a vertex in closed configuration. From this point of view, condition 1 always holds.

However, when an RPS is designed based on (3.4.6.4) tessellation, it is moveable but there is an unpredictable expansion and retraction with overlapping plates because of the assembly mode change (Fig. 12).

In mechanism science, the alternative forms that a linkage can be constructed with the same link and connections are called configurations or assembly modes of the linkages. During its motion,

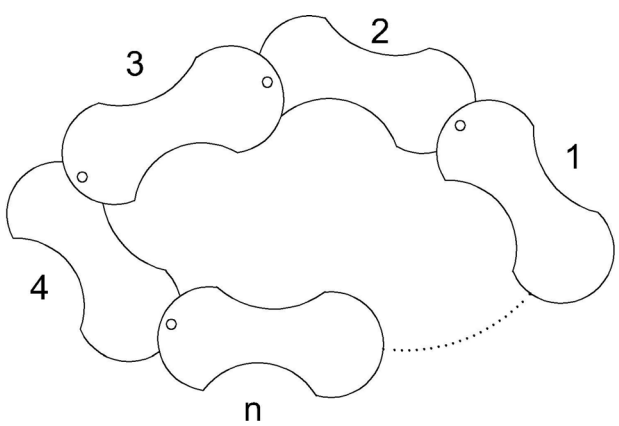

Fig. 11 Kinematic chain

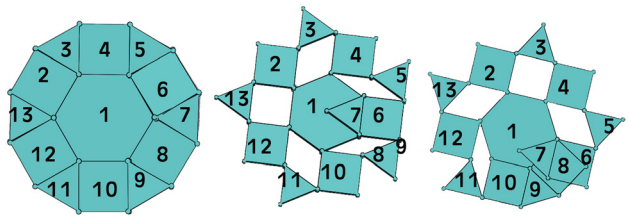

Fig. 12 Unpredictable expansion of single DoF RPS based on (3.4.6.4) tessellation

the linkage may pass from one assembly mode to another through the dead-center position, which is called reconfiguration or assembly mode change. In dead-center position, the mechanism loses its mobility and has zero mechanical advantage. The mechanism may pass easily from one configuration to another.

Above, three one-uniform tessellations are presented. All of these tessellations have four edges meeting at one vertex and they constitute parallelogram loops. Besides, one-uniform tessellations (3^2.4.3.4), (3^3.4^2), (3^4.6), (3^6) have more than four edges meeting at every vertex. RPSs based on these tessellations constitute five or six bar loops. According to Eq. (6), parameters of (3^4.6) tessellation are $L = 19$, $J_1 = 24$. The mobility of the retractable plate structure is calculated as $M = 3(19 - 1) - 2.24 = 6$. RPS is movable with an unpredictable manner because of its multi-DoF nature as shown in Fig. 13. Six DoF comes from six different pentagonal loops. In Fig. 13, it is also obvious that the number of edges meet at one vertex is equal to the number of the sides of the loops. Thus, RPS based on (3^2.4.3.4), (3^3.4^2), (3^4.6), and (3^6) tessellations can be expandable but not in a predictable manner because of having multi-DoF.

Condition 1 displays that if at least four edges meet at every vertex, it is possible to design RPSs based on these tessellations. RPS is single DoF when four edges meet at every vertex. However, single DoF RPS based on (3.4.6.4) tessellation has an unpredictable expansion with gaps or overlaps. Thus, it is necessary to have a second condition to generate RPS without any gaps or overlaps in both closed and open configurations and not interfere with each other during the deployment.

Condition 2. To reach an RPS without any gaps or overlaps in closed configuration; minimum two neighboring polygons' edges of the selected tessellation must constitute a straight line.

Proof 2. In order to prove this, let us recall the proof of condition 1 that is to be able to form a tessellation every plate should be positioned by edges to edges and corners to corners. Thus, this information reveals that every side of the polygonal plates that are the members of the tessellation should be equal to each other. In the light of this, every link in a mobile loop will be formed by the plates and its sides, in case of the smallest mobility $M = 1$ mobile loops have to be parallelograms (Fig. 14).

Due to this property, the loops will always enter their singularities (dead center position) when the edges form a straight line or when two revolute joint axes become collinear (Fig. 15). At this configuration, the system will gain a passive rotation around the collinear axis (Fig. 16) and may take infinite configuration without control possibility that will cause an unpredictable movement in the system. Moreover, mod changes can also occur during escaping this configuration (Fig. 17).

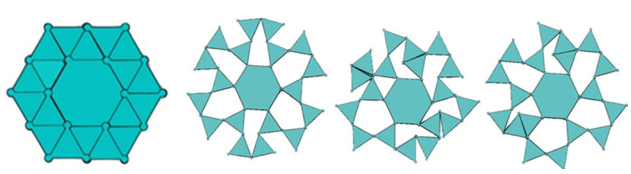

Fig. 13 Unpredictable expansion of RPS based on (3^4.6) tessellation

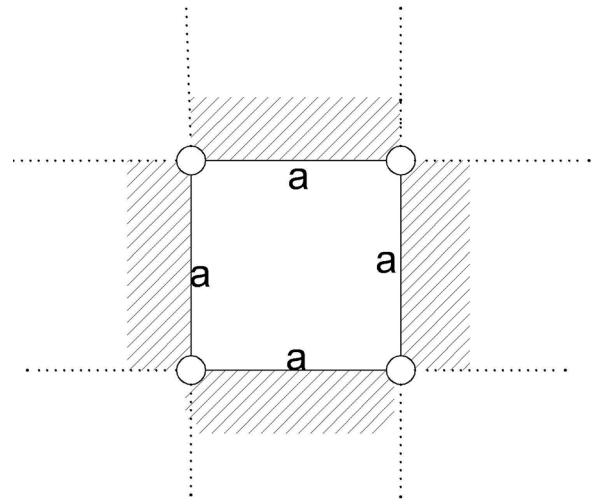

Fig. 14 $M = 1$ parallelogram loop

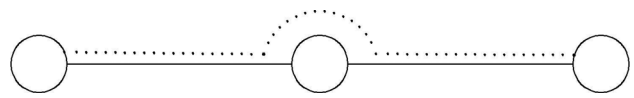

Fig. 15 Singular case of $M = 1$ parallelogram

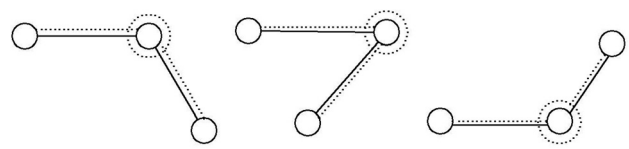

Fig. 16 Passive rotation

Using this fact, let us return to condition II. If two neighboring plates constitute a nonstraight edge connection in closed form that means their related mobile loop will enter singularity before fully closed configuration. After this point, unpredictable movements will happen and effect the movement. From this point of view, any single DoF RPS based on tessellation should conclude its closed configuration when the edges get into straight lines; thus, the condition II holds.

In order to understand the second condition, it is better to look at the kinematic behavior of the RPSs based on (4^4), (3.4.6.4), and (3.6.3.6) tessellations, which have four edges meeting at one vertex. As it is mentioned before, every four regular plates constitute parallelogram loops. During the retraction of (4^4), (3.6.3.6) tessellations, loops do not constitute a straight line. Only in fully closed configuration, loops constitute a straight line and close when the plates match perfectly. That is the dead center position of RPS.

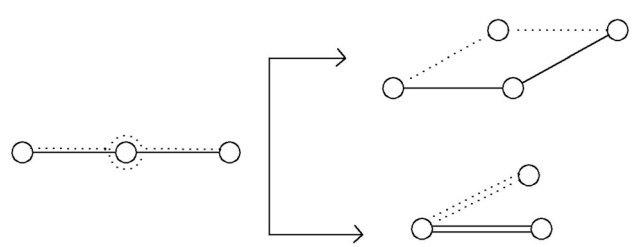

Fig. 17 Parallelogram mod-change

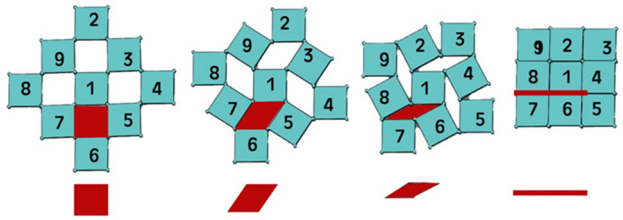

Fig. 18 Retraction and dead center position for RPS based on 4^4 tessellation

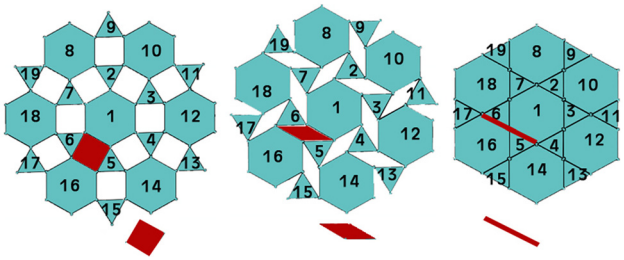

Fig. 19 Retraction and dead center position for RPS based on (3.6.3.6) tessellation

Figures 18 and 19 demonstrate the retraction capability of the RPSs based on (4^4) and (3.6.3.6) tessellations. The loops constitute straight lines when RPS reaches dead center position.

On the other hand, RPS based on (3.4.6.4) tessellation reaches dead center position before the closed configuration as in Fig. 20(*a*). In that position, parallelogram loops change the configuration easily. Thus, the movement after the dead center position is not predictable and there are overlaps as in Fig. 20(*b*). There is a relationship between the neighboring edges and behavior of the loops. Thus, it is possible to guess whether the designed RPS will have fully closed configuration or not.

Among the 11 one-uniform tessellations, it is observed that seven of tessellations (4^4), (3^6), (3.6.3.6), (3.4.6.4), (3^2.4.3.4), (3^3.4^2), (3^4.6) fulfill the condition 1 and can be retractable. However, among the seven of them, only four (4^4), (3.6.3.6), (3^4.6), (3^6) tessellations fulfill the second condition. RPS based on these can deploy without overlaps and reach closed configuration without any gaps. RPSs based on (4^4) and (3.6.3.6) tessellations are single DoF, while RPS based on (3^4.6) and (3^6) tessellations are multi-DoF.

4 Similarities Between Graph Representation and Dual of Tessellation

In many areas from engineering to architecture, graph theory is used for finding communities in networks where it is needed to detect hierarchies of substructures. In mechanism science, graph theory is generally used to employ systematic enumeration, development of computer-aided kinematics and dynamic analysis, or systematic classification of mechanisms [32,33]. In a graph representation, vertices denote links and edges denote joints of a mechanism. In a structural representation, every plate of a RPS is denoted by a polygon and its vertices represent the joints. Figure 21 displays structural and graph representations of a four bar planar mechanism that consists of four plates. It is seen that graph representation of a mechanism with four plates consists of four edges. In graph representation, a loop with four edges represents a four-bar mechanism; likewise, a loop with five edges represents a five-bar mechanism. If three plates numbered 3, 4, and 5 are assembled with 2*R* joint "*d*" as in Fig. 22, that joint is displayed with a triangle instead of a line.

The authors realize that the dual of a base tessellation is exactly the same with the graph representation of an expanded RPS. Thus, structural representation of the RPS can be easily drawn from the

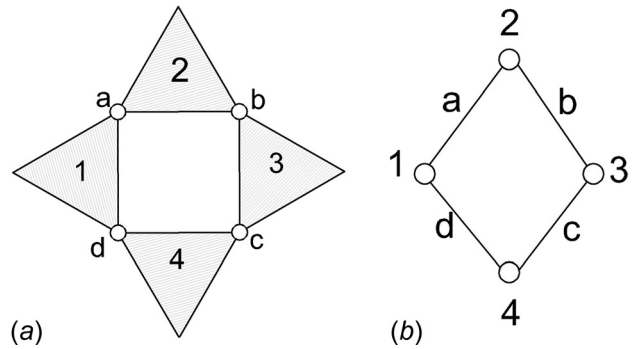

Fig. 21 (*a*) Structural representation and (*b*) graph representation

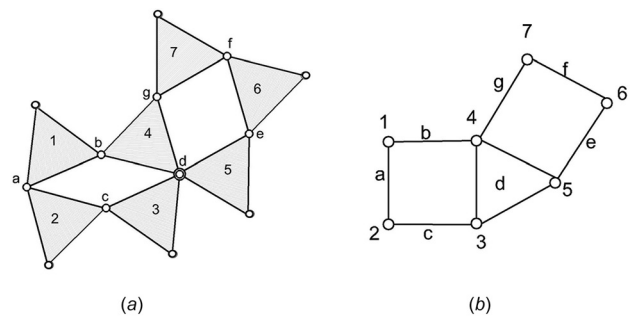

Fig. 22 (*a*) Structural representation and (*b*) graph representation

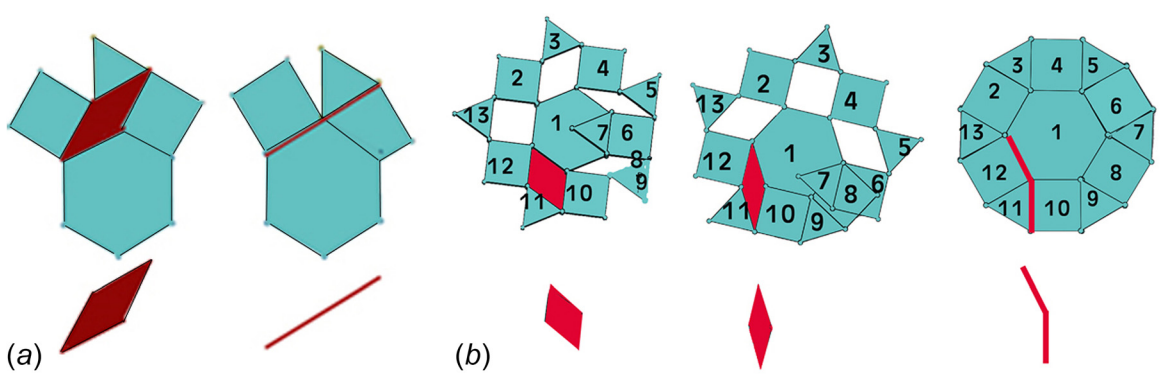

Fig. 20 (*a*) Sides of single loop reaches dead center position before fully closed configuration and (*b*) unpredictable movement of the parallelogram loops after dead center

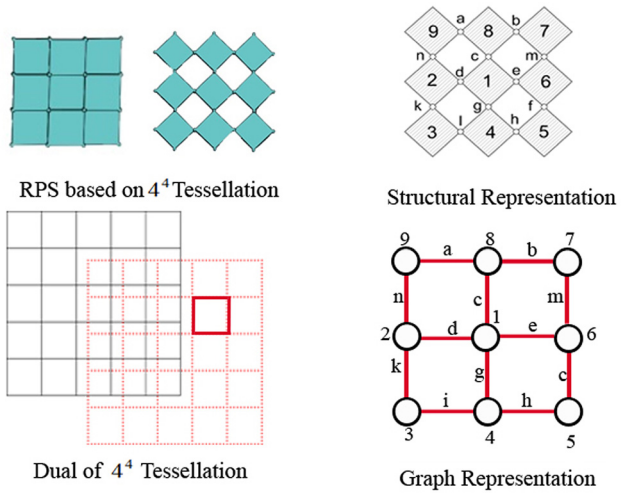

Fig. 23 Similarity between graph representation of RPS and dual of 4^4 tessellation

dual of the base tessellation. This exact similarity is shown in Figs. 23–26 for (4^4), (3.6.3.6), (3^4.6), and (3^6) tessellations. In these figures, graph representations are drawn from the structural representations of RPS and duals are drawn from the tessellations. In Figs. 23 and 24, it can be seen that duals of (4^4) and (3.6.3.6) tessellations are composed of tetragonal polygons. If the vertices are numbered and the edges are entitled on the dual, a graph of the RPS can be acquired and the structural representation of the RPS can be easily drawn from that graph. Every vertex represents a plate of RPS in graph representation. The type of the plate can be determined by counting the number of edges meeting at that vertex. If six edges meet at a vertex, that vertex represents a hexagonal plate. Moreover, since an edge on a graph represents a joint between two plates, a loop with four edges represents a four-bar mechanism and a loop with five edges represents a multi-DoF five-bar mechanism.

According to the results, a theorem can be developed from the similarities between the duality of tessellation and the graph representation of RPS.

THEOREM 1. *The dual of tessellation reveals the graph representation of RPS based on that tessellation.*

Proof 1. In order to prove theorem 1, let us consider a single module of an RPS based on that tessellation. When this module of an RPS based on a tessellation is in the fully closed form, it represents its base tessellation. In order to reveal the dual form of this tessellation, midpoints of the polygonal plates should be connected by a straight line. During this process, these lines are passing in a perpendicular fashion through the midpoints of the polygonal edges. When the same procedure is applied to the fully open-form RPS, it is easy to be seen that these straight lines will pass through the corners of the polygonal plates. As the number of corners and the numbers of edges are always the same on the polygonal plates, final geometry of whole line connections in both conditions will always be the same in different scales. Due to the fact that joints of RPS are located on the corners and they are represented as lines in the graph representation of the RPS, they will form the same geometry in fully open form when connected with the polygonal plates that are represented by dots in the graph representation. In other words, similar to the previous case, midpoints of the polygonal plates are represented by dots and connected by the lines that represented kinematic pairs. Thus, theorem 1 always holds.

5 Systematic Conversion of Multi-DoF RPS Into a Single DoF RPS

(3^4.6) and (3^6) tessellations fulfill both conditions but RPSs based on these tessellations have an unpredictable movement because of their multi-DoF nature. In this section, a systematic conversion method is presented in order to reach a single DoF RPS by using similarity between the duality of tessellations and the graph representation of expanded RPS.

Main purpose of this method is to generate tetragonal polygons on the dual of tessellations manually. In the light of this idea, tetragonal loops will be generated by either adding extra edges or

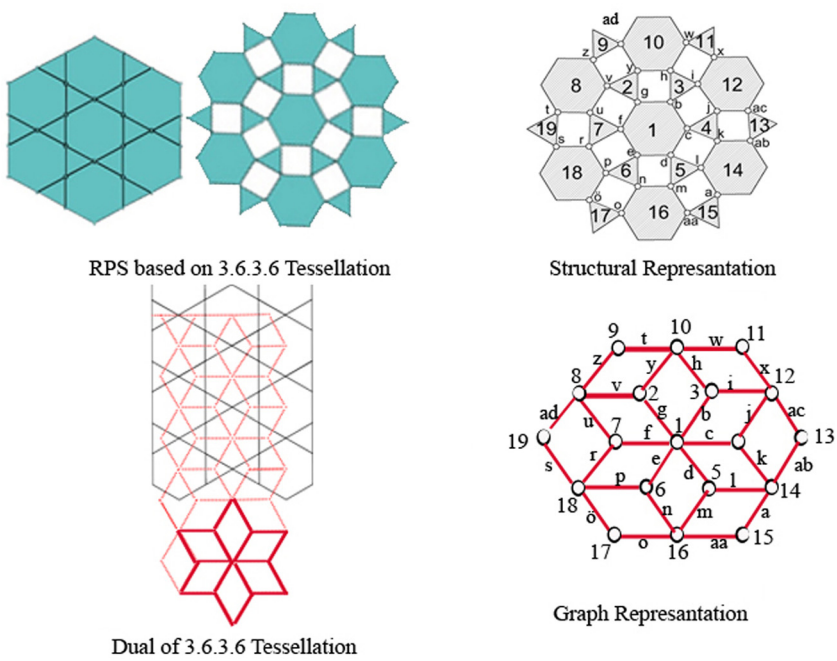

Fig. 24 Similarity between graph representation of RPS and dual of 3.6.3.6 tessellation

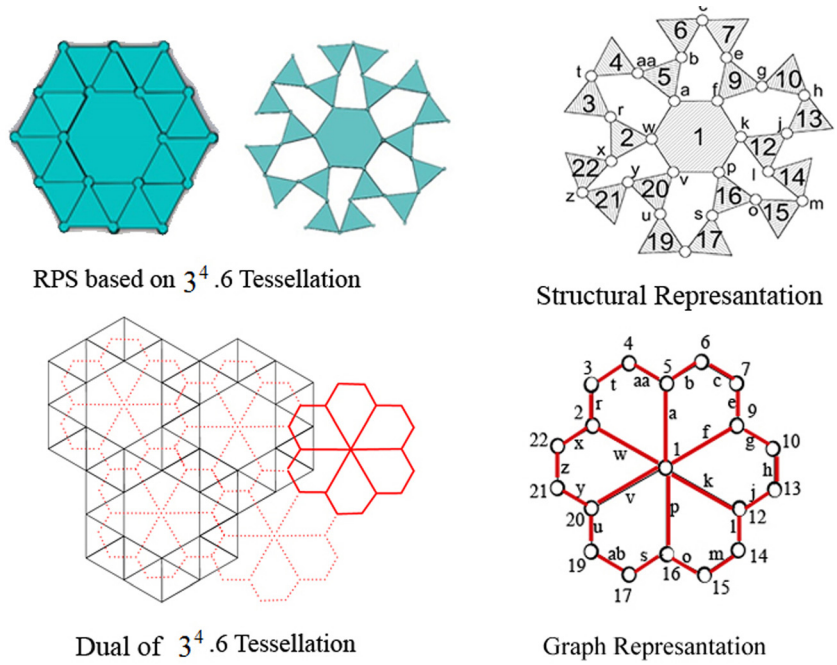

Fig. 25 Similarity between graph representation of RPS and dual of $3^4.6$ tessellation

points into the graph representation. As it is mentioned before, an edge refers to a joint and a point refers to a plate. Indeed, this method will reveal the idea of how the plates should be assembled. The method will be explained through the creation of a single DoF RPS based on (3^4.6) tessellation.

Step 1: Acquiring the dual of the base tessellation

As a first step, the dual of (3^4.6) tessellation is drawn. Black lines show (3^4.6) tessellation while the red lines show its dual as in Fig. 27. It can be seen that the dual of (3^4.6) tessellation consists of five-sided polygons. Thus, if the plates are assembled one by one with revolute joints, the graph representation of an expanded RPS based on (3^4.6) tessellation will consist of five-sided polygons, which represents multi-DoF loops. It is revealed that RPS based on (3^4.6) tessellation will be multi-DoF.

Step 2: Modification of the dual of base tessellation

As a second step, extra edges are added to the dual of tessellation in order to generate tetragonal polygons as in Fig. 28. The new form is the graph representation of the RPS. An extra edge in graph represents the assembly of two plates with an extra joint.

Step 3: Focusing on to the key points of graph representation

In the process of drawing the graph representation from the dual of tessellation, two important points should be considered. The first one is to avoid generating a subchain or an overconstrained subchain. While drawing new edges on the dual to

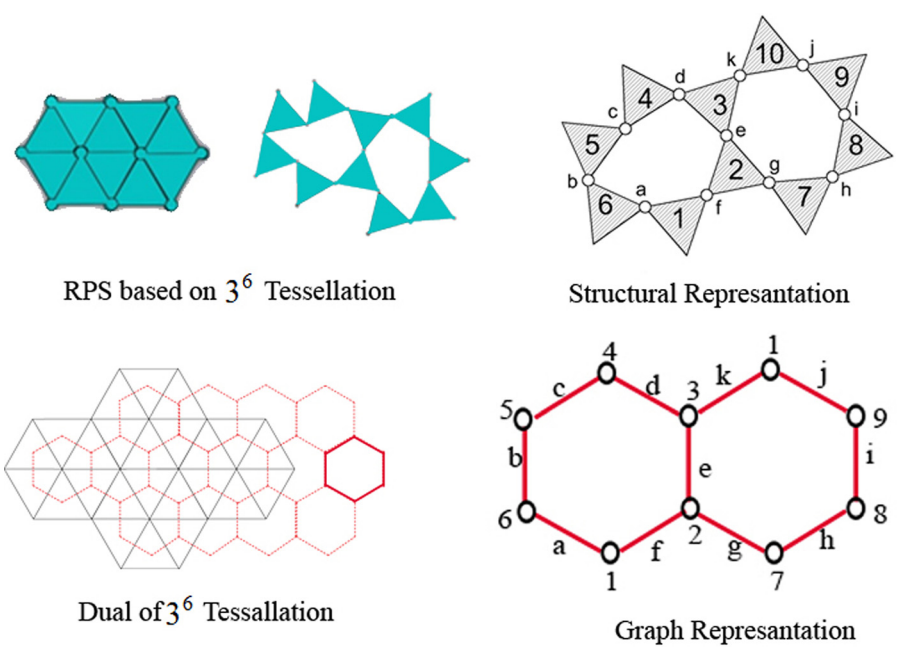

Fig. 26 Similarity between graph representation of RPS and dual of 3^6 tessellation

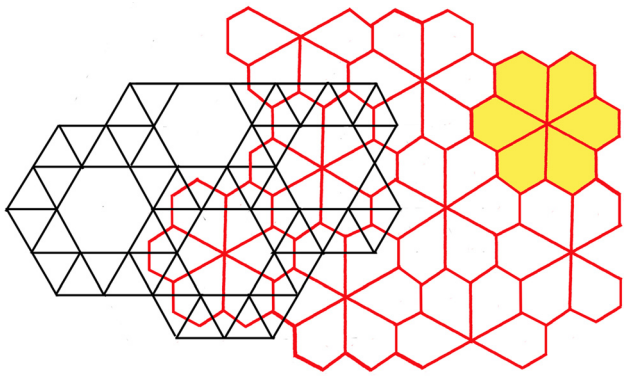

Fig. 27 $3^4.6$ tessellation and its dual

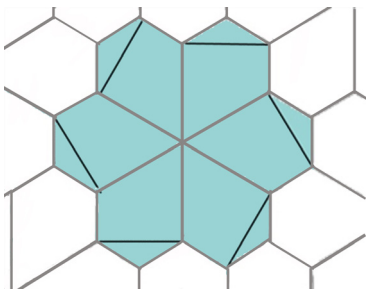

Fig. 28 Modification of the dual of base tessellation

generate tetragonal polygons, it is also possible to generate new triangular polygons. As it is represented in Fig. 29, a triangle denotes a subchain in graph representation. The plates numbered 1, 2, and 3 generate a triangular loop when assembled with revolute joints lettered *a*, *b*, and *f*. They generate a structure as shown in Fig. 30. Besides, it is not possible to connect plates numbered 5 and 1. In addition to this, if two triangles lettered *a* and *b* are drawn side by side they, represent 2*R* joints as in Fig. 31. Thus, plates numbered 2 and 3 generate an overconstrained subchain as in Fig. 32 and these two plates move as a single body.

The second important point is the number of edges that meet at every vertex. On a graph representation, if three edges meet at one vertex, it is a triangular plate with three joints, if six edges meet at one vertex, it is a hexagonal plate with six joints. While drawing new edges on a dual of tessellation, the number of edges that meet at one vertex should be carefully counted with respect to the chosen tessellation's polygon types. For instance, Fig. 33 shows a

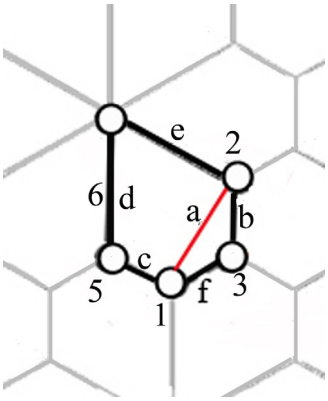

Fig. 29 Graph representation of a subchain creation

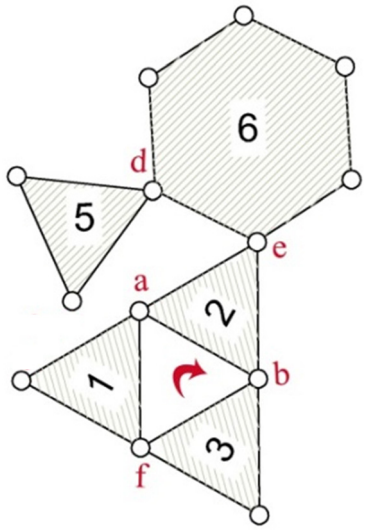

Fig. 30 Structural representation a subchain

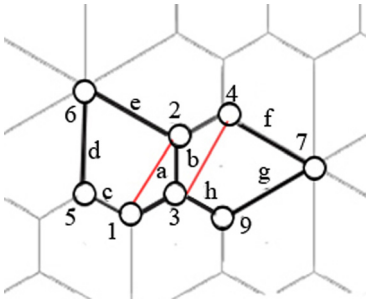

Fig. 31 Graph representation of an over constraint subchain creation

graph representation after drawing new edges to the dual of $3^4.6$ tessellation. The plate "3" has two 2*R* joints lettered *a* and *b*. However, RPS based on $3^4.6$ tessellation should have plates with three *R* joints or with six *R* joints to be connected with neighboring plates. As it seen in Fig. 34, the plate numbered 3 is not a regular triangular link any more. The link is connected with two 2*R* joints (*a* and *b*) instead of three *R* joints.

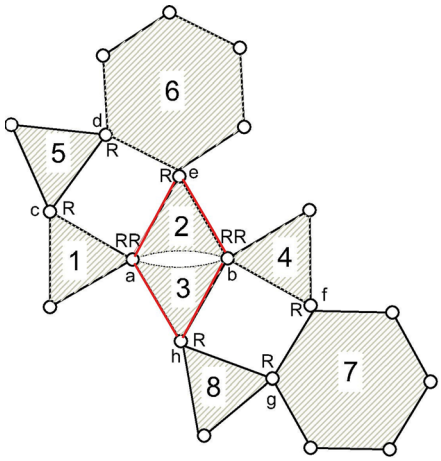

Fig. 32 Structural representation with over constrained subchain

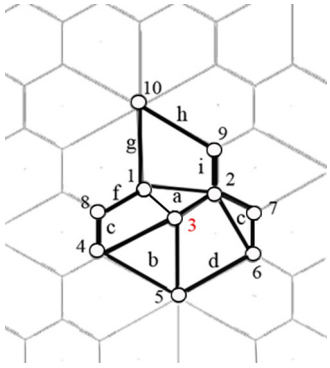

Fig. 33 Graph representation

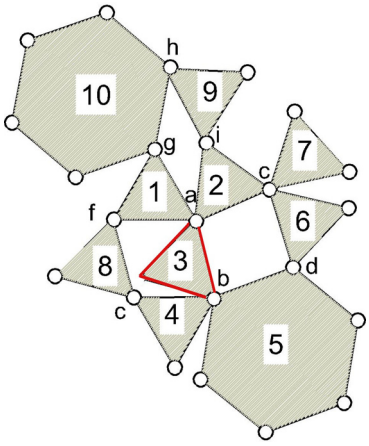

Fig. 34 Structural representation

Figure 35 shows a correct graph representation of RPS module where the vertices are numbered and the edges are lettered. Triangular plates are connected to neighboring plates with three joints that are R or $2R$ joints.

Step 4: Assembly of the plates and RPS construction

Structural representation of RPS is drawn according to the graph representation. From the graph, it is understood that plates numbered 1, 30, 33, 34, 35, 36, and 37 are hexagonal; others are triangular plates. Rigid plates are assembled with revolute joints as in Fig. 36 according to the generated graph representation.

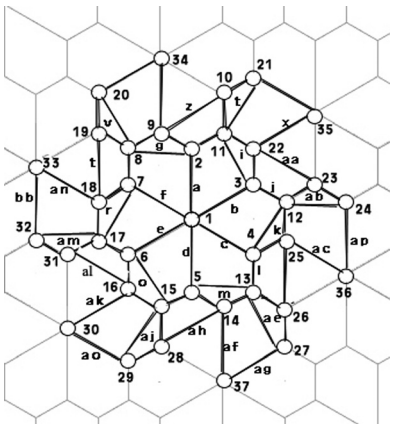

Fig. 35 Graph representation of the RPS module without any subchain

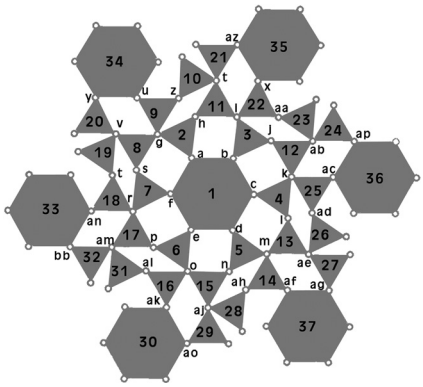

Fig. 36 Structural representation of RPS module

In Fig. 37, it can be seen that a single DoF RPS module based on (3^4.6) tessellation can be designed by connecting two plates with new joints. It can expand and retract in a predictable manner without any gaps or overlaps.

In Fig. 38, black lines show the generated graph representation of the module, while the red lines show the edges drawn from vertices 30, 33, 34, 35, 36, and 37 to the neighboring vertices to iterate the graph. These new edges drawn to the dual create six triangles on graph representation. Triangle on graph represents a subchain or a $2R$ joints. If RPS is constructed with subchains numbered (34,10,9), (33,19,18), (31,16,30), (28,14,37), (26,25,36), and (23,22,35), only one subchain is enough to prevent the movement. If RPS is constructed with six extra R joints, the plates numbered 28, 31, 19, 10, 23, and 26 have two $2R$ joints, respectively, (aj, af), (am, al), (t, v), (z, t) (aa, ab) (ae, ac) instead of three R joints. These plates are not triangular with three R joints. Because of these reasons, the iteration of the module is not possible.

The only way to iterate the graph representation is to generate overconstrained subchains. Figure 39 shows the graph representation of RPS where the overconstrained subchains are drawn in order to create four-sided polygons on the dual tessellation. However, as it is mentioned before, overconstrained subchains cause two plates to move as a single tetragonal plate. Figure 40 shows the structural representation and Fig. 41 shows the expansion of the new RPS.

On the other hand, when this method is applied to RPS based on 3^6 tessellation by considering the key points, subchains or overconstrained subchains are always generated with extra edges as in Fig. 42. Besides, the number of joints on the triangular plates will be more or less than three. For example, plate number 42 has four joints and plate numbered 59 has two joints. It is obvious that the graph representation of a single DoF RPS cannot be drawn only by adding extra edges to the dual.

In order to draw a graph representation consisting of tetragonal polygons, both extra vertices and edges should be drawn on the dual. As seen in Fig. 43, black points display the vertices of the dual while blue points display the newly added vertices. A new graph is generated by drawing the edges between all vertices as in Fig. 44. The graph is generated after vertices are numbered and edges are lettered as in Fig. 45. It is seen that six edges meet at

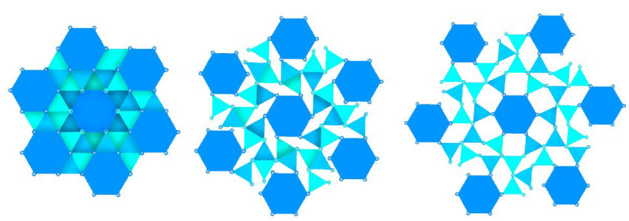

Fig. 37 Expansion of a RPS module based on 3^4.6 tessellation

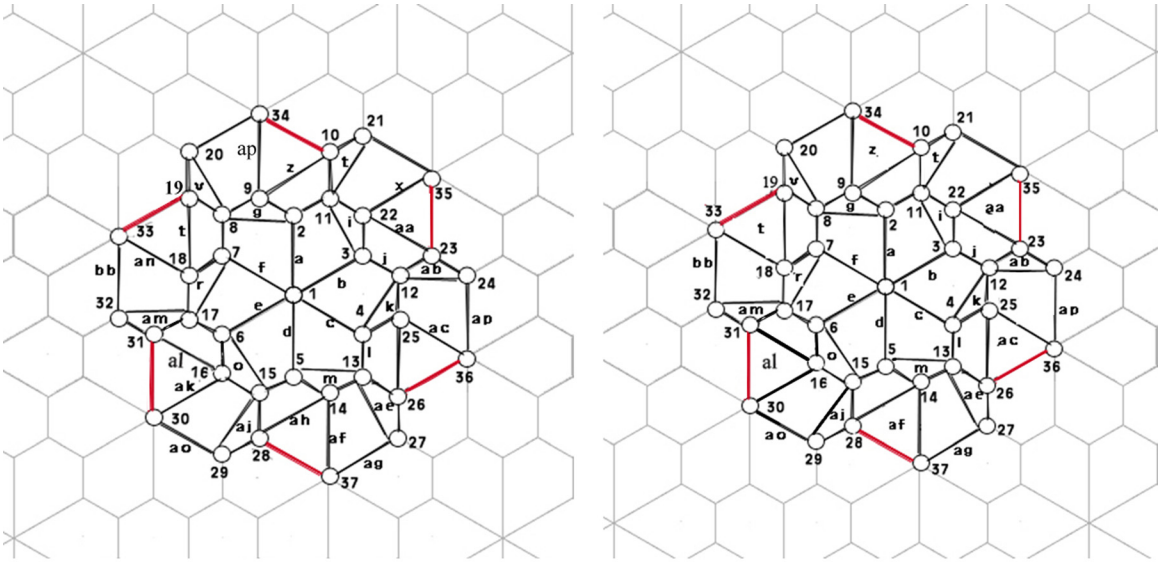

(*a*) (*b*)

Fig. 38 (*a*) Graph representation with six subchains and (*b*) with six extra 2*R* joints

new vertices, which represent hexagonal extra plates with six revolute joints and three edges meet at vertices of the dual, which represent triangular plates with three revolute joints. The new single DoF RPS based on 3^6 tessellation consists of triangular plates but is connected with extra hexagonal plates in order to create parallelogram loops as in Fig. 46.

6 Conclusion

This paper presents a novel family of single DoF RPSs that can be expanded and retracted without any gaps or overlaps in both open and closed configurations. In order to find the shape of hinged plates, a new approach using tessellation technique is used. This study restricted with one-uniform tessellations that are 11 different tiling possibilities of regular polygons. Two conditions are determined to design a RPS, which expands and retracts in a predictable manner from these 11 tiling.

By connecting the regular polygonal plates through revolute joints, it is observed that single or multi-DoF RPS modules are acquired. The authors discovered a similarity between dual of the base tessellation and the graph representation of the RPS. This

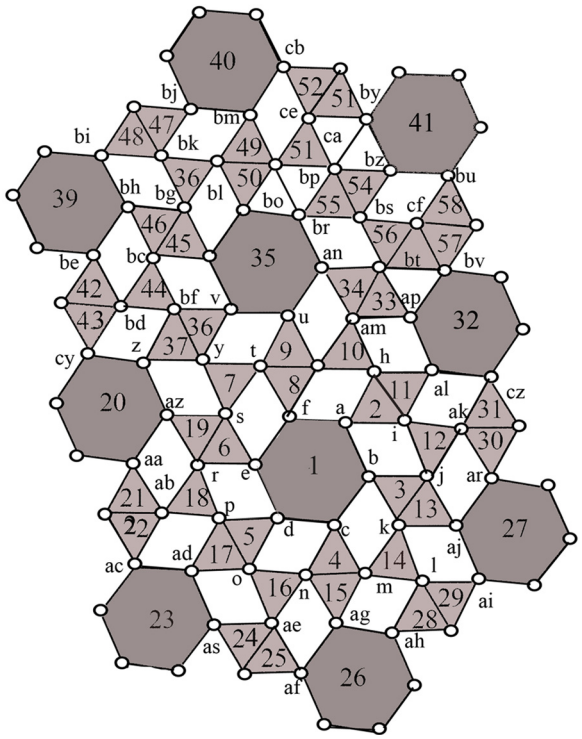

Fig. 40 Structural representation based on $3^4.6$ tessellation by generating overconstrained subchains

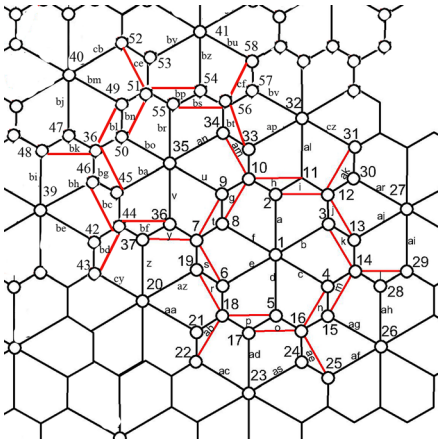

Fig. 39 Graph representation based on $3^4.6$ tessellation by generating overconstrained subchains

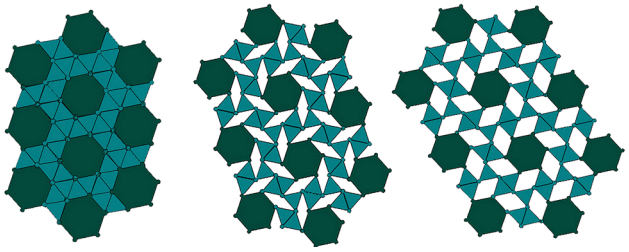

Fig. 41 Expansion of iterated RPS based on $3^4.6$ tessellation by generating overconstrained subchain

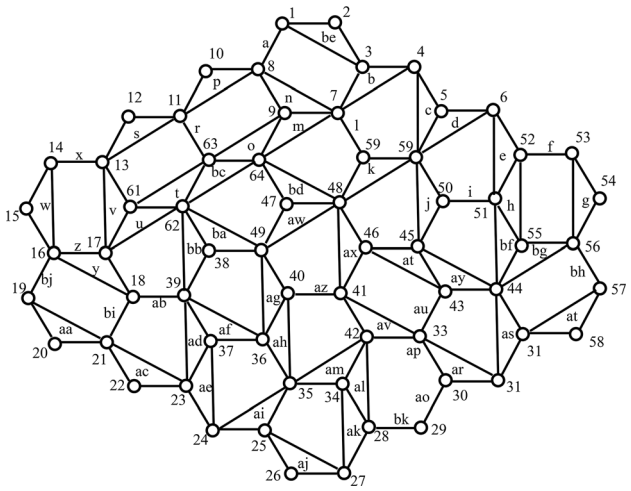

Fig. 42 Attempt to draw graph representation of RPS based on 3^6 tessellations

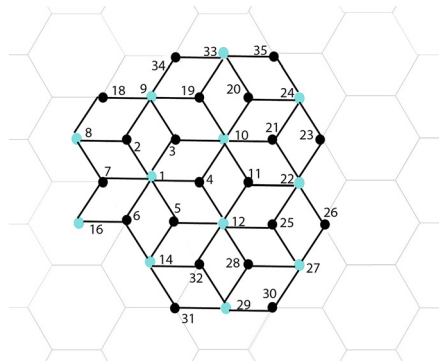

Fig. 44 Drawing tetragons on the dual

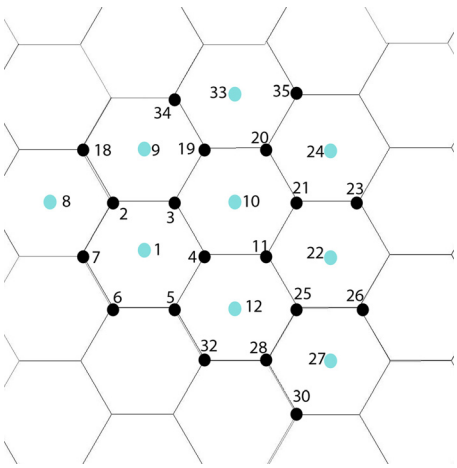

Fig. 43 Addition of extra points to the dual

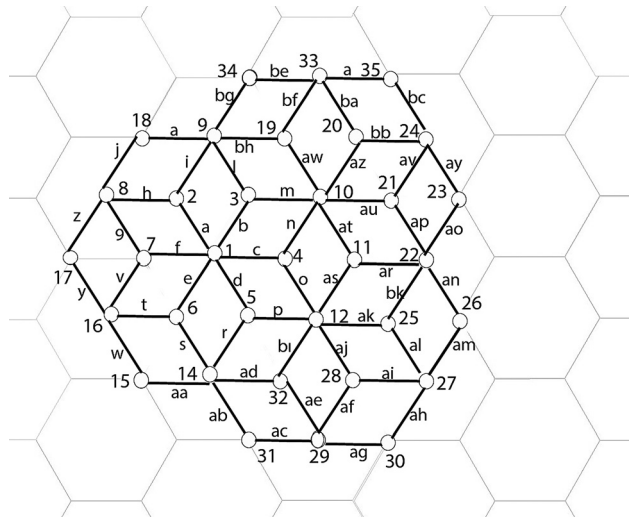

Fig. 45 Graph representation of RPS based on 3^6 tessellation

similarity is used in the design process and a method is explained step by step in order to convert multi-DoF RPS into a single DoF RPS.

Developed conditions and theorems have been made available to the architects and engineers to design retractable plate structures without having any complex engineering or mathematical knowledge. Thus, these results present potential advantage for the applications of retractable plate structures to architectural projects more than today.

One of the most important factor that must be considered in deployable scissor structures is the covering material. In general, flexible materials able to follow the deployment of the scissor structure are required. By replacing the bars with plates, RPSs appear to be more or less suitable for certain functions in the façade or on the roof a building such as solar shading devices. This paper gives a first impression on the applicability of retractable plate structure to a responsive building skin as in Fig. 47.

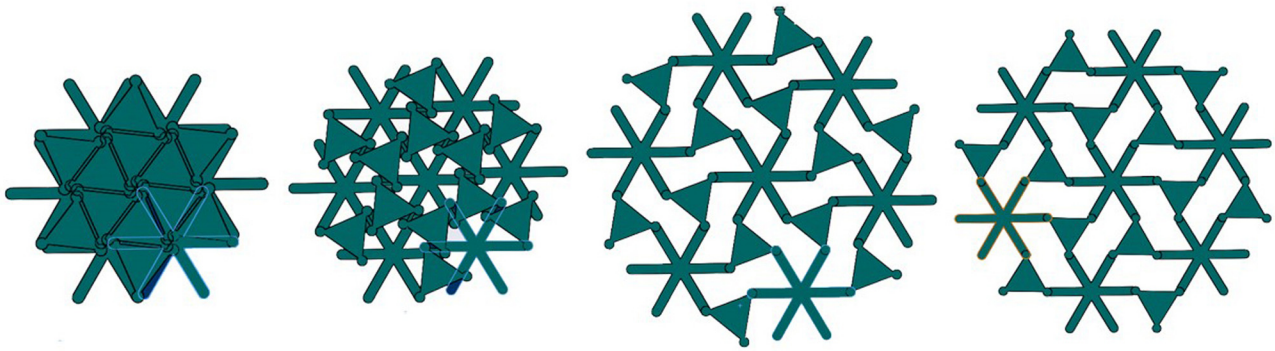

Fig. 46 Expansion of RPS based on 3^6 tessellation

Fig. 47 Application of a RPS to a building

References

[1] Ishii, K., 2000, *Structural Design of Retractable Roof Structures*, WIT Press, Southampton, UK.

[2] Hoberman, C., 1991, "Radial Expansion Retraction Truss Structure," U.S. Patent No. 5,024,031.

[3] Sharif, S., Gentry, T., Yen, J., and Goodman, J., 2013, "Transformative Solar Panels: A Multidisciplinary Approach," Int. J. Archit. Comput., **11**(2), pp. 227–246.

[4] Piñero, E. P., and Escrig Pallarés, F., 1993, *Arquitectura Transformable*, Escuela Técnica Superior de Arquitectura de Sevilla, Sevilla, Spain.

[5] Escrig, F., and Valcarcel, J. P., 1993, "Geometry of Expandable Space Structures," Int. J. Space Struct., **8**(1–2), pp. 71–84.

[6] Hoberman, C., 1990, "Reversibly Expandable Doubly-Curved Truss Structures," U.S. Patent No. 4,942,700.

[7] You, Z., and Pellegrino, S., 1997, "The Universal Scissor Component: Optimization of a Reconfigurable Component for Deployable Scissor Structures," Eng. Optim., **48**(2), pp. 317–333.

[8] Mira, L. A., 2009–2010, "Design and Analysis of Universal Scissor Components for Mobile Architectural Applications," M.Sc. thesis, Vrije Univeriteit, Brussels, Belgium.

[9] Kassabian, P., You, Z., and Pellegrino, S., 1999, "Retractable Roof Structures," Proc. Inst. Civ. Eng. Struct. Build., **134**(2), pp. 45–56.

[10] Jensen, F., and Pellegrino, S., 2002, "Expandable Structures Formed by Hinged Plates," Space Struct., **5**(1), pp. 263–272.

[11] Jensen, F., and Pellegrino, S., 2005, "Expandable 'BloB' Structures," J. Int. Assoc. Shell Spat. Struct., **46**(3), pp. 151–158.

[12] Lou, Y., Mao, D., and You, Z., 2007, "On a Type of Radially Retractable Plate Structures," Int. J. Solids Struct., **44**(10), pp. 3452–3467.

[13] Rodriquez, C., and Chilton, J., 2003, "Swivel Diaphragm a New Alternative for Retractable Ring Structure," J. Int. Shell Spat. Struct., **44**(3), pp. 181–188.

[14] Wohlhart, K., 2000, "Double-Chain Mechanisms," *IUTAM-IASS Symposium on Deployable Structures: Theory and Applications*, S. Pellegrino and S. Guest, eds., Kluwer Academic Publishers, Dordrecht, The Netherlands, pp. 457–466.

[15] Wei, G., and Dai, J. S., 2014, "A Spatial Eight-Bar Linkage and Its Association With the Deployable Platonic Mechanisms," ASME J. Mech. Rob., **6**(2), p. 021010.

[16] Wei, G., Chen, Y., and Dai, J. S., 2014, "Synthesis, Mobility, and Multifurcation of Deployable Polyhedral Mechanisms With Radially Reciprocating Motion," ASME J. Mech. Des., **136**(9), p. 091003.

[17] Gazi, A., and Korkmaz, K., 2015, "8.8.4 Tesselasyon Kullanarak Genisleyebilen Strüktür Tasarimi," Uluslararası Katılımlı 17. Makina Teorisi Sempozyumu, pp. 441–442.

[18] Gazi, A., and Korkmaz, K., 2015, "Design Method for Radially Retractable Single DOF Plate Structure Based on Regular 1-Uniform Regular Tessellation," Megaron, **10**(3), pp. 317–331.

[19] Sareh, P., and Guest, S. D., 2015, "A Framework for the Symmetric Generalization of the Miura-Ori," Int. J. Space Struct., **30**(2), pp. 141–152.

[20] Sareh, P., and Guest, S. D., 2015, "Design of Isomorphic Symmetric Descendants of the Miura-Ori," IOP J. Smart Mater. Struct., **24**(8), pp. 1–12.

[21] Seymour, D., and Britton, J., 1989, *Introduction to Tessellations*, Dale Seymour Publications, Palo Alto, CA.

[22] Kepler, J., 1619, *Harmonice Mundi Lincii*, Lincii Austriæ, Sumptibus G. Tampachii, Excudebat I. Plancvs.

[23] Sommerville, D. M. Y., 1905, "Semi-Regular Networks of the Plane in Absolute Geometry," Trans. - R. Soc. Edinburgh, **41**, pp. 725–759.

[24] Kinsey, L. C., and Moore, T. E., 2002, *Symmetry, Shape and Space: An Introduction to Mathematics Through Geometry*, Key College Publishing, New York.

[25] Grünbaum, B., and Shephard, G., 1984, *Tilings and Patterns*, W. H. Freeman and Company, New York.

[26] Krötenheerdt, O., 1969, "Die Homogenen Mosaike n-ter Ordnung in der Euklidischen Ebene," Doctoral dissertation, Wiss. Z. Martin Luther-University Halle-Wittenberg, Halle, Germany.

[27] Phillips, J., 2006, *Freedom in Machinery*, Cambridge University Press, Cambridge, UK.

[28] Dai, J. S., Huang, Z., and Lipkin, H., 2004, "Screw System Analysis of Parallel Mechanisms and Applications to Constraint and Mobility Study," ASME Paper No. DETC2004-57604.

[29] Dai, J. S., Huang, Z., and Lipkin, H., 2006, "Mobility of Overconstrained Parallel Mechanisms," ASME J. Mech. Des., **128**(1), pp. 220–229.

[30] Wei, G., Ding, X., and Dai, J. S., 2010, "Mobility and Geometric Analysis of the Hoberman Switch-Pitch Ball and Its Variant," ASME J. Mech. Rob., **2**(3), p. 031010.

[31] Alizade, R., Bayram, C., and Gezgin, E., 2007, "Structural Synthesis of Serial Platform Manipulators," Mech. Mach. Theory, **42**(5), pp. 580–599.

[32] Tsai, L. W., 2001, *Mechanism Design Enumeration of Kinematic Structure According to Function*, CRC Press, Boca Raton, FL.

[33] Feng, C. M., and Liu, T. S., 2013, "A Graph-Theory Approach to Designing Deployable Mechanism of Reflector Antenna," Acta Astronaut., **87**, pp. 40–47.